arXiv:1512.01813v1 [math.OC] 6 Dec 2015

A residual based snapshot location strategy for POD in distributed optimal control of linear parabolic equations

A. Alla * **C. Gräßle** * **M. Hinze** *

* *Universität Hamburg, Bundesstr. 55, 20146, Hamburg, Germany (e-mail: {alessandro.alla, carmen.graessle, michael.hinze}@uni-hamburg.de).*

Abstract: In this paper we study the approximation of a distributed optimal control problem for linear parabolic PDEs with model order reduction based on Proper Orthogonal Decomposition (POD-MOR). POD-MOR is a Galerkin approach where the basis functions are obtained upon information contained in time snapshots of the parabolic PDE related to given input data. In the present work we show that for POD-MOR in optimal control of parabolic equations it is important to have knowledge about the controlled system at the right time instances. For the determination of the time instances (snapshot locations) we propose an a-posteriori error control concept which is based on a reformulation of the optimality system of the underlying optimal control problem as a second order in time and fourth order in space elliptic system which is approximated by a space-time finite element method. Finally, we present numerical tests to illustrate our approach and to show the effectiveness of the method in comparison to existing approaches.

Keywords: Optimal Control, Model Order Reduction, Proper Orthogonal Decomposition, Snapshot Location.

1. INTRODUCTION

Optimization with PDE constraints is nowadays a well-studied topic motivated by its relevance in industrial applications. We are interested in the numerical approximation of such optimization problems in an efficient and reliable way using surrogate models obtained with POD-MOR. The surrogate models in the present work are in general built upon snapshot information of the system. This idea was introduced in Sirovich (1987).

Several works focus their attention on the choice of the snapshots in order to approximate either dynamical systems or optimal control problems by suitable surrogate models. Here we mention the work related to the computation of the snapshots for dynamical system in Kunisch et al. (2010) and Hoppe et al. (2014).

In optimal control problems the reduced model is usually built upon a forecast on the control which in general does not guarantee a proper construction of the surrogate model, since one does not know how far away the optimal solution is from this forecast control. More sophisticated approaches select snapshots by solving an optimization problem in order to improve the selection of the snapshots according to the desired controlled dynamics. For this purpose optimality system POD (shortly OS-POD) is introduced in Kunisch et al. (2008). Adaptive adjustments of the surrogate models are proposed in Afanasiev et al. (2001) and in Arian et al. (2002). In our paper, we address the question of efficient selection of snapshot locations by means of an a-posteriori error control approach proposed in Gong et al. (2012), where the optimality system is rewritten as a second order in time and a fourth order in space elliptic equation. In particular, the time-adaptivity is used to build the snapshot grid which should be used to construct the POD-MOR surrogate model for the approximate solution of the optimal control problem. Here the contribution for the reduced control problem is twofold: we directly obtain snapshots related to an approximation of the optimal control and, at the same time, obtain information about the time grid.

The outline of this paper is as follows. In Section 2 we present the optimal control problem together with the optimality conditions. In Section 3 we present the main results of Gong et al. (2012). POD and its application to optimal control problems is presented in Section 4. Here, we explain our strategy for snapshot location. Finally, numerical tests are discussed in Section 5. A conclusion and outlook are given in Section 6.

2. OPTIMAL CONTROL PROBLEM

In this section we describe the distributed optimal control problem. The governing equation is given by

$$\left.\begin{aligned} y_t - \nu\Delta y &= f + u && \text{in } \Omega_T,\\ y(\cdot,0) &= y_0 && \text{in } \Omega,\\ y &= 0 && \text{on } \Sigma_T, \end{aligned}\right\} \tag{1}$$

where ν, T are given real positive constants, $\Omega_T := \Omega \times (0,T]$, $\Omega \subset \mathbb{R}^n$ is an open bounded domain with smooth

⋆ We would like to thank Z J. Zhou, from Shandong Normal University, China, for providing the data and code of the space-time approximation in Gong et al. (2012).

boundary, $\Sigma_T := \partial\Omega \times (0,T]$. The state and the control are denoted by $y : \Omega_T \to \mathbb{R}$ and $u : \Omega_T \to \mathbb{R}$, respectively. We note that (1) for $y_0 \in L^2(\Omega)$ and $u \in L^2(0,T;H^{-1}(\Omega))$ admits a unique solution $y = y(u) \in W(0,T)$, where

$$W(0,T) := \left\{ v \in L^2\left(0,T;H_0^1(\Omega)\right), \frac{\partial v}{\partial t} \in L^2\left(0,T;H^{-1}(\Omega)\right) \right\}.$$

The cost functional we want to minimize is given by

$$J(y,u) := \frac{1}{2}\|y - y_d\|^2_{L^2(\Omega_T)} + \frac{\alpha}{2}\|u\|^2_{L^2(\Omega_T)}, \qquad (2)$$

where $y_d \in L^2(\Omega_T)$ is the desired state and α is a real positive constant. The optimal control problem, then, can be formulated as

$$\min_{u \in L^2(\Omega_T)} J(y(u),u) \text{ where } y(u) \text{ satisfies (1).} \qquad (3)$$

It is easy to argue that (3) admits a unique solution $u \in L^2(\Omega_T)$ with associated state $y(u) \in W(0,T)$, see e.g. Tröltzsch (2010).

The optimality system of the optimal control problem (3) is given by the state equation (1) together with the adjoint equation

$$\left.\begin{aligned} -p_t - \nu\Delta p &= y - y_d && \text{in } \Omega_T,\\ p(\cdot,T) &= 0 && \text{in } \Omega,\\ p &= 0 && \text{on } \Sigma_T, \end{aligned}\right\} \qquad (4)$$

and the optimality condition

$$\alpha u + p = 0 \quad \text{in } \Omega_T. \qquad (5)$$

Since our domain is smooth, the regularities of the optimal state, the optimal control and the associated adjoint state are limited through the regularities of the initial state y_0 and of the desired state y_d.

The numerical approximation of the optimality system (1)-(4)-(5) with a standard Finite Element Method (FEM) leads to a high-dimensional boundary value problem with respect to time:

$$\left.\begin{aligned} M\dot{y}^N - \nu A y^N &= f^N + u^N, \quad && y^N(0) = y_0^N.\\ -M\dot{p}^N - \nu A p^N &= y^N - y_d^N, \quad && p^N(T) = 0.\\ \alpha u^N + p^N &= 0 \end{aligned}\right\} \qquad (6)$$

Here $y^N, p^N : [0,T] \to \mathbb{R}^N$ are the semi-discrete state and adjoint, respectively, $\dot{y}^N$ is the time derivative, $M \in \mathbb{R}^{N\times N}$ denotes the finite element mass matrix and $A \in \mathbb{R}^{N\times N}$ the finite element stiffness matrix. Note that the dimension N of each equation in the semi-discrete system (6) is related to the number of element nodes chosen in the FEM approach.

3. SPACE-TIME APPROXIMATION

In this section we transform the first order optimality conditions (1)-(4)-(5) into an elliptic equation of fourth order in space and second order in time involving only the state variable y. The interested reader can find more details on this section in Gong et al. (2012). Here, we recall the main results.

Under natural assumptions the optimality system (1)-(4)-(5) may be rewritten as a boundary value problem in space-time:

$$\left.\begin{aligned} -y_{tt} + \nu\Delta^2 y + \frac{1}{\alpha}y &= \frac{1}{\alpha}y_d && \text{in } \Omega_T,\\ y(\cdot,0) &= y_0 && \text{in } \Omega,\\ y &= 0 && \text{on } \Sigma_T,\\ \Delta y &= 0 && \text{on } \Sigma_T,\\ (y_t - \Delta y)(T) &= 0 && \text{in } \Omega. \end{aligned}\right\} \qquad (7)$$

Here we set $f \equiv 0$. In Gong et al. (2012), under suitable assumptions on the data, it is shown that the solution to problem (3) satisfies (7) almost everywhere in space time. Next we provide the weak formulation of (7). For this purpose let:

$$H_0^{2,1}(\Omega_T) := \left\{ v \in H^{2,1}(\Omega_T) : v(0) = 0 \text{ in } \Omega \right\},$$

where

$$H^{2,1}(\Omega_T) := L^2\left(0,T;H^2(\Omega)\cap H_0^1(\Omega)\right)\cap H^1\left(0,T;L^2(\Omega)\right),$$

and is equipped with the norm

$$\|w\|^2_{H^{2,1}(\Omega_T)} := \left(\|w\|^2_{L^2(0,T;H^2(\Omega))} + \|w\|^2_{H^1(0,T;L^2(\Omega))}\right).$$

The bilinear form and the linear form in the weak formulation are defined as:

$$A_T : H_0^{2,1}(\Omega_T)\times H_0^{2,1}(\Omega_T) \to \mathbb{R}, \qquad L_T : H_0^{2,1}(\Omega_T) \to \mathbb{R},$$

$$\begin{aligned} A_T(v,w) &:= \int_{\Omega_T}\left(v_t w_t + \frac{1}{\alpha}vw\right)\\ &\quad + \int_{\Omega_T}\Delta v\Delta w + \int_\Omega \nabla v(T)\nabla w(T),\\ L_T(v) &:= \int_{\Omega_T}\frac{1}{\alpha}y_d v. \end{aligned}$$

The weak formulation of equation (7) then reads: given $y_d \in L^2(\Omega_T)$, $y_0 \in H_0^1(\Omega)$, find $y \in H^{2,1}(\Omega_T)$ with $y(0) = y_0$ and

$$A_T(y,v) = L_T(v) \quad \forall v \in H_0^{2,1}(\Omega_T). \qquad (8)$$

Existence and uniqueness of the solution is proved e.g. in Neitzel et al. (2009) and Gong et al. (2012).

We put our attention on the discrete approximation of (7). As a first step we recall a-priori and a-posteriori error estimates for the semi-discrete problem, where the space is kept continuous. Let us consider the time discretization $0 = t_0 < t_1 < \ldots < t_n = T$ with $\Delta t_j = t_j - t_{j-1}$ and $\Delta t := \max_j \Delta t_j$. Let $I_j := [t_{j-1}, t_j]$, we define

$$V_t^k := \left\{ v \in H^{2,1}(\Omega_T) : \ v(x,\cdot)|_{I_j} \in P_1(I_j) \text{ for a.e. } x \in \Omega \right\},$$

and

$$\bar{V}_t^k := V_t^k \cap H_0^{2,1}(\Omega_T).$$

We now consider the semi-discrete problem

$$A_T(y_k, v_k) = L_T(v_k), \quad \forall v_k \in \bar{V}_t^k. \qquad (9)$$

Under suitable assumptions on the data we have the following a-priori error estimate from (Gong et al., 2012, Thm 3.1):

$$\|y - y_k\|_{L^2(\Omega_T)} + \Delta t\|y - y_k\|_{H^1(0,T;L^2(\Omega))} \le C\Delta t^2.$$

Furthermore, from (Gong et al., 2012, Thm 3.3) we also have the temporal a posteriori error estimate

$$\|y - y_k\|^2_{H_0^{2,1}(\Omega_T)} \le C\eta^2, \qquad (10)$$

where

$$\eta^2 = \sum_j \Delta t_j^2 \int_{I_j} \|\frac{1}{\alpha} y_d + \frac{\partial^2 y_k}{\partial t^2} - \frac{1}{\alpha} y_k - \Delta^2 y_k\|^2_{L^2(\Omega)} + \sum_j \int_{I_j} \|\Delta y_k\|^2_{L^2(\Gamma)}. \quad (11)$$

With the help of (10), we are able to refine the time grid by means of the residual of the system (7). The snapshot selection for POD-MOR of problem (3) will now be based on (10).

4. POD FOR OPTIMAL CONTROL PROBLEMS

In this section we explain the POD method which we utilize in order to replace the original (high-dimensional) problem (3) by a (low-dimensional) POD-Galerkin approximation. The main interest when applying the POD method is to reduce calculation times and storage capacity while retaining a satisfactory approximation quality. This is made possible due to the key fact that POD basis functions contain information about the underlying model, since the POD basis are derived from snapshots of a solution data set. For this reason it is important to use rich snapshot ensembles reflecting the dynamics of the modelled system. The snapshot form of POD proposed by Sirovich (1987) works in the discrete version as follows. Let us suppose that the continuous solution $y(t)$ of (1) belongs to a real separable Hilbert space V, equipped with the inner product $\langle \cdot, \cdot \rangle$. In fact, in the applications we use either $V = L^2(\Omega)$ or $V = H_0^1(\Omega)$. For given time instances $t_0, t_1, \ldots, t_n$ we suppose to know the solution $y(t_j)$ of (1) for $j = 0, \ldots, n$. We define the snapshot set $\mathcal{V} := \text{span}\{y(t_0), \ldots, y(t_n)\} \subset V$ and determine a POD basis $\{\psi_1, \ldots, \psi_\ell\}$ of rank $\ell \in \{1, ..., d\}, d = \dim \mathcal{V} \leq N$, by solving the following minimization problem:

$$\min_{\psi_1,\ldots,\psi_\ell \in \mathbb{R}^N} \sum_{j=0}^{n} \beta_j \left\| y(t_j) - \sum_{i=1}^{\ell} \langle y(t_j), \psi_i \rangle \, \psi_i \right\|^2 \quad \text{s.t. } \langle \psi_j, \psi_i \rangle = \delta_{ij} \quad \text{for } 1 \leq i, j \leq \ell, \quad (12)$$

where β_j are nonnegative weights and δ_{ij} denotes the Kronecker symbol. The associated norm is given by $\|\cdot\|^2 = \langle \cdot, \cdot \rangle$.

It is well-known (see e.g. Gubisch et al. (2013)) that a solution to problem (12) is given by the first ℓ eigenvectors $\{\psi_1, \ldots, \psi_\ell\}$ corresponding to the ℓ largest eigenvalues λ_i of the self-adjoint linear operator $\mathcal{R} : V \to V$, i.e. $\mathcal{R}\psi_i = \lambda_i \psi_i$ with $\lambda_i > 0$, where $\mathcal{R}$ is defined as follows:

$$\mathcal{R}\psi = \sum_{j=0}^{n} \beta_j \langle y(t_j), \psi \rangle \, y(t_j) \quad \text{for } \psi \in V.$$

Moreover, we can quantify the POD approximation error by the neglected eigenvalues depending on the snapshots (more details can be found in e.g. Gubisch et al. (2013)) as follows:

$$\sum_{j=0}^{n} \beta_j \left\| y(t_j) - \sum_{i=1}^{\ell} \langle y(t_j), \psi_i \rangle \, \psi_i \right\|^2 = \sum_{i=\ell+1}^{d} \lambda_i. \quad (13)$$

Let us assume we are able to compute POD basis functions for the optimal control problem (3). Then, we define the POD ansatz of order ℓ for the state y as

$$y^\ell(t) = \sum_{i=1}^{\ell} w_i(t) \psi_i, \quad (14)$$

where $y^\ell \in V^\ell \subset V$, the POD basis functions are $\{\psi_i\}_{i=1}^\ell$ and the unknown coefficients are $\{w_i\}_{i=1}^\ell$. If we plug this assumption into (1) we get the following reduced system

$$M^\ell \dot{w} - \nu A^\ell w = u^\ell, \quad w(0) = w_0, \quad (15)$$

where entries of the mass matrix M^ℓ and the stiffness matrix A^ℓ are given by $(M^\ell)_{ij} = \langle \psi_j, \psi_i \rangle$ and $(A^\ell)_{ij} = \langle \nabla \psi_i, \nabla \psi_j \rangle$, respectively. The coefficients of the initial condition $y^\ell(0) \in \mathbb{R}^\ell$ are determined by $w_i(0) = (w_0)_i = \langle y_0, \psi_i \rangle, \quad 1 \leq i \leq \ell$, and the projected desired state is obtained as $(w_d)_i = \langle y_d, \psi_i \rangle, 1 \leq i \leq \ell$.

Thus, the optimal control problem of reduced order is obtained through replacing (3) by a dynamical system obtained from a Galerkin approximation with modes $\{\psi_i\}_{i=1}^\ell$ and ansatz (14) for the state variable. This POD-Galerkin approximation leads to the optimization problem

$$\min_{u \in L^2(\Omega_T)} \hat{J}^\ell(u) \text{ s.t. } y^\ell(u) \text{ satisfies (15)}, \quad (16)$$

where $\hat{J}^\ell$ is the reduced cost functional, i.e. $\hat{J}^\ell(u) := \hat{J}(y^\ell(u), u)$. We recall that the discretization of the optimal solution $\bar{u}^\ell$ to (16) is determined by the relation between the adjoint state and control and refer to Hinze (2005) for more details about this variational discretization concept.

Now let us draw our attention to our *snapshot location* strategy for POD model order reduction in optimal control. Recalling the minimization problem (12), we observe the strong dependence of the POD basis functions on the chosen snapshots. These snapshots shall have the property to capture the main features of the dynamics of the truth solution as good as possible. Here, we face some difficulties since the reduction of optimal control problems is usually initialized with snapshots computed from a given input control u_{sg} ('u_{sg}': control input for **s**napshot **g**eneration). In general, we do not have any information about the optimal control, so that in POD-MOR often $u_{\text{sg}} \equiv 0$ is chosen.

The a-posteriori error control concept for (7) now offers the possibility to select snapshot locations by a time-adaptive procedure. For this purpose, (7) is solved adaptively in time, where the spatial resolution (Δx in Algorithm 1) is chosen very coarse. The resulting time grid points now serve as snapshot locations, on which our POD-MOR model for the optimization is based, where the snapshots are now obtained from a simulation of (1) with high spatial resolution h. The right-hand side u is obtained from (5) with p from (4) computed with spatially coarse resolution. The procedure is summarized in Algorithm 1.

5. NUMERICAL TEST

In our numerical computations we use a one-dimensional spatial domain and a finite element discretization in space by means of conformal piecewise linear polynomials with an implicit Euler discretization in time. The coefficients β_j in (12) are chosen according to the trapezoidal rule. All coding is done in MATLAB R2015a, and the computations are performed on a 2.50GHz computer.

Algorithm 1 Adaptive snapshot selection for optimal control problems.

Require: coarse spatial grid size Δx, fine spatial grid size h, max number of degrees of freedom (dof) for the adaptive time discretization, $T > 0$.

1: Solve (7) adaptively w.r.t. time with spatial resolution Δx and obtain time grid $\mathcal{T}$ with solution $y_{\Delta x}$.
2: Solve (4) on $\mathcal{T}$ with spatial resolution Δx and r.h.s. $y_{\Delta x}$ to obtain $p_{\Delta x}$. Set $u = -\frac{1}{\alpha} p_{\Delta x}$.
3: Solve (1) on $\mathcal{T}$ with spatial resolution h and r.h.s. u extended to the spatial grid with resolution h.
4: Compute a POD basis of order ℓ and build the POD-MOR model.
5: Solve (16) with time grid $\mathcal{T}$ and POD-MOR model (15).

In the following numerical test, we apply the adaptive snapshot selection strategy of Algorithm 1 to demonstrate which influence the chosen time grid can have on the approximation quality of the POD suboptimal solution and compare with results obtained on an equidistant time grid.

Test Example 5.1. The data for this test example is taken from Example 5.2 in Gong et al. (2012), where the following choices are made: $\Omega = (0,1)$ and $[0,T] = [0,1]$. We set $\alpha = 1$ and $\nu = 1$. The example is built in such a way that the exact optimal solution $(\bar{y}, \bar{u})$ of problem (3) with associated optimal adjoint state $\bar{p}$ is known:

$$\bar{y}(x,t) = \sin(\pi x)\operatorname{atan}\left(\frac{t-1/2}{\varepsilon}\right),$$

$$\bar{u}(x,t) = -\sin(\pi x)\sin(\pi t),\ \bar{p}(x,t) = \sin(\pi x)\sin(\pi t).$$

The initial condition is $y_0(x) = \sin(\pi x)\operatorname{atan}(-1/(2\varepsilon))$, f and y_d are chosen accordingly. For small values of ε (we use $\varepsilon = 10^{-3}$), the state $\bar{y}$ develops an interior layer at $t = 1/2$, which can be seen at the top of Figure 1 and Figure 2.

The main focus of our investigation consists in the use of two different types of time grids: an equidistant time grid characterized by the time increment $\Delta t = 1/n$ and a non-equidistant (adaptive) time grid characterized by $n+1$ degrees of freedom (dof). Figure 3 visualizes the space-time mesh resulting from the strategy of Gong et al. (2012) utilizing temporal a-posteriori error estimation. The first grid in Figure 3 corresponds to the choice dof $= 21$ and $\Delta x = 1/100$, whereas the grid in the middle refers to using dof $= 21$ and $\Delta x = 1/5$. Both choices for spatial discretization lead to the exact same time grid, which displays fine time steps at time $t = 1/2$ (where the layer in the optimal state is located), whereas at the beginning and end of the time interval the time steps are large. This clearly indicates that the resulting time-adaptive grid is very insensitive against changes in the spatial resolution. As a consequence we expect that the time grid obtained with a very coarse spatial resolution already delivers a time grid which well suits for the selection of fully resolved time-snapshots of the state, which form the basis of our POD-MOR strategy. For the sake of completeness, the equidistant grid with the same number of degrees of freedom is displayed at the bottom of Figure 3.

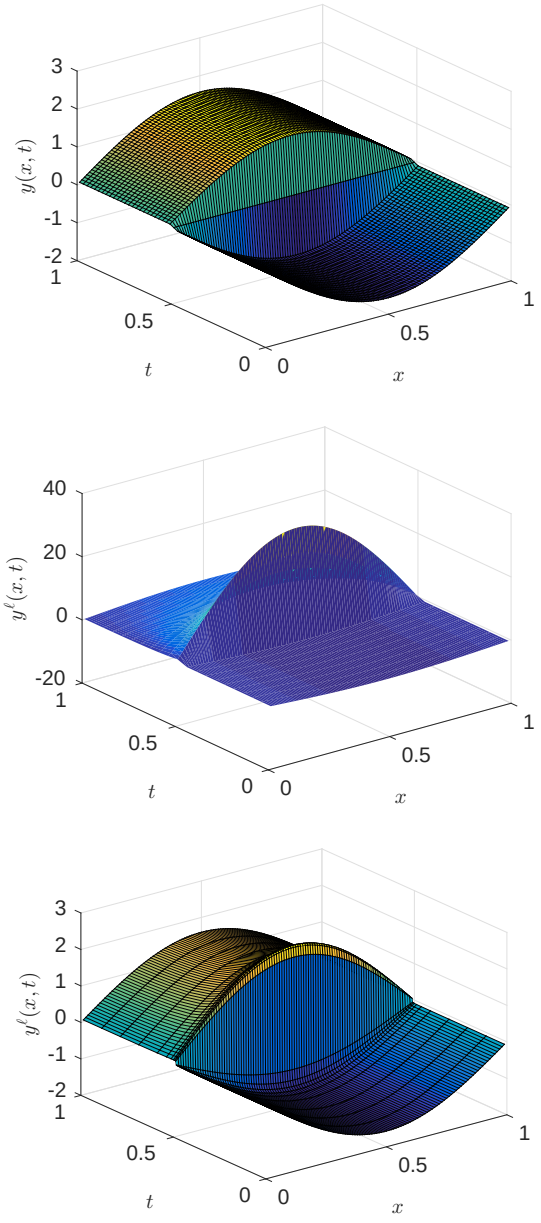

Fig. 1. Exact optimal state $\bar{y}$ (top), approximated POD solution computed on an equidistant time grid (middle), approximated POD solution utilizing the adaptive time grid (bottom)

Since the generation of the time-adaptive grid as well as the approximation of the optimal solution is done in the offline computation part of POD-MOR, this process shall be performed quickly, which is why we pick $\Delta x = 1/5$ for step 1 in Algorithm 1. For the computation of a POD suboptimal solution we make the following choices: we use uncontrolled snapshots, i.e. we create the snapshot ensemble by determining the associated state $y(u_{\mathrm{sg}})$ to the control function $u_{\mathrm{sg}} \equiv 0$. Although we would also have the possibility to use snapshots associated to a spatially coarse optimal control (since this optimal control is computed within Algorithm 1), we want to emphasize here the importance of the time grid and compare with the most common snapshot selection approach in practice. Moreover, we use 1 POD basis function determined by the MATLAB routine

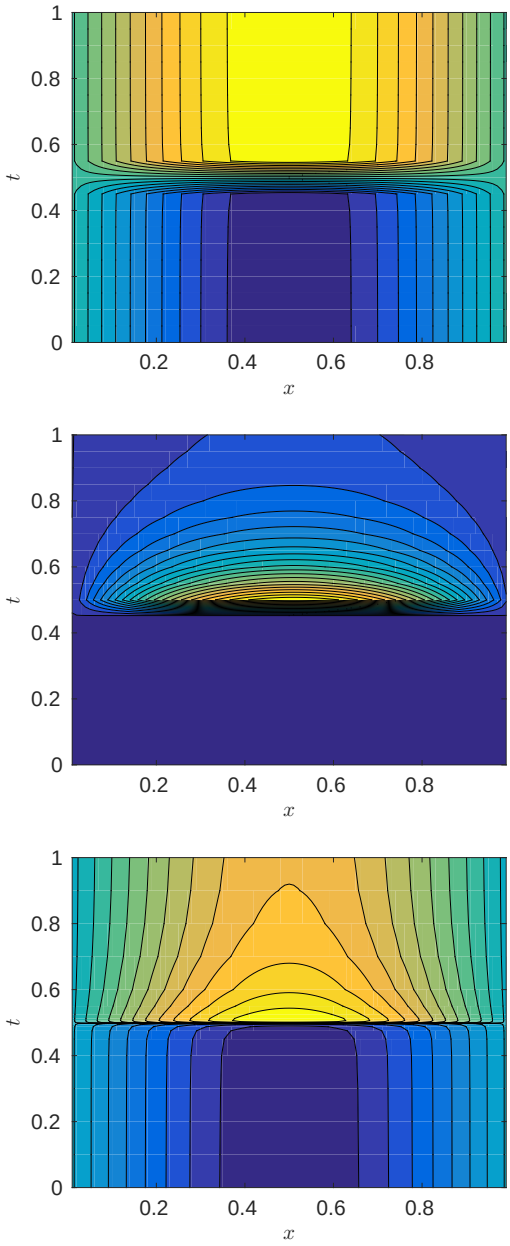

Fig. 2. Contour lines of the exact optimal state $\bar{y}$ (top), the approximated POD solution computed on an equidistant time grid (middle), the approximated POD solution utilizing the adaptive time grid (bottom)

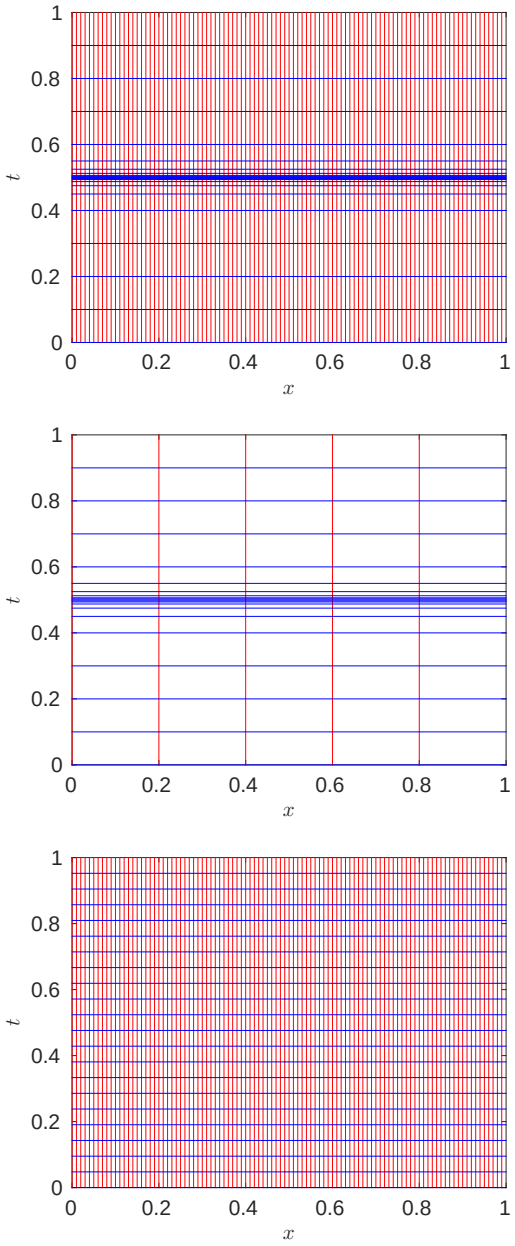

Fig. 3. Adaptive space-time grids with dof = 21 according to the strategy in Gong et al. (2012) and $\Delta x = 1/100$ (top) and $\Delta x = 1/5$ (middle), respectively, and the equidistant grid (bottom) with $\Delta x = 1/100$ and $\Delta t = 1/20$

`eigs`, i.e. $\ell = 1$. As weighted inner product we choose $\langle v, w\rangle = \langle v, Ww\rangle_{\mathbb{R}^N}$ with $W = M$, where N refers to the dimension of the finite element space associated with the spatial grid size h.

Table 1 and Table 2 summarize all test runs with an equidistant and adaptive time grid, respectively. The fineness of time discretization is chosen in such a manner that the results are comparable. The absolute errors between the exact optimal state $\bar{y}$ and the POD suboptimal solution $\bar{y}^\ell$, defined by $\varepsilon^y_{\text{abs}} := \| \bar{y} - \bar{y}^\ell \|_{L^2(\Omega_T)}$, are listed in columns 2, same applies for the absolute errors in the control function, $\varepsilon^u_{\text{abs}} := \| \bar{u} - \bar{u}^\ell \|_{L^2(\Omega_T)}$, columns 3. If we compare the errors between exact and POD solution utilizing an equidistant time grid with the results for the errors utilizing the adaptive time grid, we clearly notice that the use of an adaptive time grid heavily improves the quality of the numerical POD solution.

In fact, our numerical tests enable us to detect the following: in order to achieve an accuracy in the state variable of order 10^{-1} utilizing an equidistant time grid, we need about $n = 110$ time steps and for an accuracy of order 10^{-2} about $n = 400$ time steps are needed (not listed in Table 1). Once again, this emphasizes that using an appropriate (non-equidistant) time grid is of particular importance in order to efficiently achieve POD solutions of good quality.

Figures 1 and 2 (middle and bottom plots) show the surface and contour lines of the POD suboptimal state uti-

Δt	$\varepsilon^y_{\text{abs}}$	$\varepsilon^u_{\text{abs}}$
1/20	$6.7264 \cdot 10^{+00}$	$4.7581 \cdot 10^{-01}$
1/46	$2.8634 \cdot 10^{+00}$	$1.9863 \cdot 10^{-01}$
1/82	$1.4603 \cdot 10^{+00}$	$1.0037 \cdot 10^{-01}$
1/108	$1.0233 \cdot 10^{+00}$	$6.9951 \cdot 10^{-02}$

Table 1. Absolute errors between the exact optimal solution and the POD suboptimal solution depending on the time discretization with equidistant grid

dof	$\varepsilon^y_{\text{abs}}$	$\varepsilon^u_{\text{abs}}$
21	$1.8468 \cdot 10^{-01}$	$1.1610 \cdot 10^{-02}$
47	$2.0049 \cdot 10^{-02}$	$9.3412 \cdot 10^{-03}$
83	$1.2574 \cdot 10^{-02}$	$5.0596 \cdot 10^{-03}$
109	$6.3950 \cdot 10^{-03}$	$4.8042 \cdot 10^{-03}$

Table 2. Absolute errors between the exact optimal solution and the POD suboptimal solution depending on the time discretization with adaptive grid

lizing an equidistant time grid (with $\Delta t = 1/20$) and utilizing the adaptive time grid (with dof = 21), respectively. As expected, significant differences can be noticed in the appearance: an equidistant time grid fails to capture the interior layer at $t = 1/2$ satisfactorily, whereas the POD solution utilizing the adaptive time grid approximates the interior layer well.

We note that enlarging the number of utilized POD basis functions does not improve the approximation quality. Furthermore, we can argue that the percentage of modelled energy to total energy contained in the snapshots (energy content) is approximately 1.00 and the second largest eigenvalue of the correlation matrix is of order 10^{-16} (machine precision), which makes the use of additional POD basis functions redundant. Likewise, as already mentioned, in this particular example the choice of richer snapshots (even the optimal snapshots) does not bring significant improvements in the approximation quality of the POD solutions. So, this example shows that solely the use of an appropriate adaptive time mesh effectively improves the accuracy of the POD suboptimal solution.

The last remark goes to the efficiency of the POD method. For the solution of the full-dimensional problem, 4 iterations of the gradient method are needed, which means the approximation of 8 (high-dimensional) PDEs is required, whereas the reduced model took 5 iterations implying the approximation of 10 ODEs of dimension $\ell = 1$. The offline stage is really cheap since we use a very coarse spatial discretization.

6. CONLCUSION AND FUTURE DIRECTIONS

In this paper we investigate the problem of snapshot location in optimal control problems. We show that the numerical POD solution is much more accurate if we use an adaptive time grid, especially when the solution of the problem presents layers. The time grid is computed by means of an a-posteriori error estimation strategy of the space-time approximation of a second order in time and fourth space elliptic equation which describes the optimal control problem and has the advantage that it does not explicitly depend on an input control function. Furthermore, a coarse approximation of the latter equation gives information on the snapshots one can use to build the surrogate model. Future work will focus on error analysis of the proposed algorithm, and on optimal control with shape functions and control constraints.

REFERENCES

K. Afanasiev and M. Hinze. Adaptive control of a wake flow using proper orthogonal decomposition. *Lecture Notes in Pure and Applied Mathematics 216*, 317-332. Shape Optimization & Optimal Design, Marcel Dekker, 2001.

E. Arian, M. Fahl and E. Sachs. Trust-region proper orthogonal decomposition models by optimization methods. *In Proceedings of the 41st IEEE Conference on Decision and Control, Las Vegas, Nevada*, pages 3300-3305, 2002.

W. Gong, M. Hinze, Z.J.Zhou. Space-time finite element approximation of parabolic optimal control problems. *J. Numer. Math*, **20**, 2012, 111-145.

M. Gubisch and S. Volkwein. Proper Orthogonal Decomposition for Linear-Quadratic Optimal Control. *Submitted*, 2013.

K. Kunisch, S. Volkwein. Galerkin proper orthogonal decomposition methods for parabolic problems. *Numer. Math.* 90 (2001), 117-148.

K. Kunisch, S. Volkwein. Galerkin proper orthogonal decomposition methods for a general equation in fluid dynamics. *SIAM, J. Numer. Anal.* **40** (2002), 492-515.

K. Kunisch and S. Volkwein. Proper Orthogonal decomposition for optimality systems. *ESAIM: M2AN,* **42**, 2008, 1-23.

K. Kunisch and S. Volkwein. Optimal Snapshot Location for computing POD basis functions. *ESAIM: M2AN,* **44**, 2010, 509-529.

M. Hinze. A variational discretization concept in control constrained optimization: the linear-quadratic case. *Computational Optimization and Applications,* 30, 45-61, 2005

M. Hinze, R. Pinnau, M. Ulbrich and S. Ulbrich. Optimization with PDE Constraints. Mathematical Modelling: Theory and Applications, 23. *Springer Verlag,* 2009.

R.H.W. Hoppe and Z. Liu. Snapshot location by error equilibration in proper orthogonal decomposition for linear and semilinear parabolic partial differential equations *J. of Numer. Math.,* **22**, 2014, 1-32.

I. Neitzel, U. Prüfert, T. Slawig. On Solving Parabolic Optimal Control Problems by Using Space-Time Discretization. *Technical Report* 05-2009, TU Berlin

J. Nocedal and S.J. Wright. Numerical Optimization, second edition. *Springer Series in Operation Research and Financial Engineering,* 2006.

L. Sirovich. Turbulence and the dynamics of coherent structures. Parts I-II. *Quarterly of Applied Mathematics,* **XVL** (1987), 561-590.

F. Tröltzsch. Optimal Control of Partial Differential Equations: Theory, Methods and Application. *American Mathematical Society,* 2010.

F. Tröltzsch and S. Volkwein. POD a-posteriori error estimates for linear-quadratic optimal control problems. *Comput. Optim. and Appl.,* **44**, 2009, 83-115.